This article has been accepted for publication in a future issue of this journal, but has not been fully edited. Content may change prior to final publication. Citation information: DOI 10.1109/TIE.2015.2399277, IEEE Transactions on Industrial Electronics

MPPT with Single DC-DC Converter and Inverter for Grid Connected Hybrid Wind-Driven PMSG-PV System

M. M. Rajan Singaravel and S. Arul Daniel

***Abstract*--A new topology of a hybrid distributed generator based on photovoltaic and wind-driven permanent magnet synchronous generator is proposed. In this generator, the sources are together connected to the grid with the help of only a single boost converter followed by an inverter. Thus, compared to earlier schemes, the proposed scheme has fewer power converters. Model of the proposed scheme in *d-q* axes reference frame is developed. Two low cost controllers are also proposed for the new hybrid scheme to separately trigger the DC-DC converter and the inverter for tracking the maximum power from both the sources. The integrated operations of both the proposed controllers for different conditions are demonstrated through simulation and experimentation. Steady-state performance of the system and transient response of the controllers are also presented to demonstrate the successful operation of the new hybrid system. Comparison of experimental and simulation results are given to validate the simulation model.**

***Index Terms*—Hybrid Distributed Generators, Wind-driven PMSG-PV, Grid connected hybrid system, Smart grid**

NOMENCLATURE

V_{OC}	Open Circuit Voltage of PV array (V)
V_S	PMSG stator voltage (V)
V_b, V_{DC}	Boost converter output voltage (V)
V_R	Rectifier output voltage (V)
V_{pv}	PV array terminal voltage (V)
V_m	Maximum power point voltage of PV array (V)
V_{GRID}	Output voltage of the inverter (V)
v_{Gd}, v_{Gq}	d-axis and q-axis voltage of grid (V)
v_d, v_q	d-axis and q-axis voltage of inverter (V)
E	Stator EMF of PMSG (V)
I_{SC}	Short circuit current of PV array (A)
I_S	PMSG stator current (A)
I_R	Rectifier output current (A)
I_b	Boost converter output current (A)
I_{DC}	DC link current (A)
I_{GRID}	Output current of the inverter (A)
I_{pv}	Current from PV array (A)
I_d	Current through internal diode of PV array (A)
I_m	PV array current at maximum power point (A)
i_d, i_q	d-axis and q-axis current of inverter (A)
I_{ref}	Reference current signal for inverter (A)
R_{se}	Series resistance of PV array (Ω)
X_s	PMSG stator reactance (Ω)
δ	Duty-cycle of the boost converter
L_f	Filter inductor at inverter output (mH)

Manuscript received September 17, 2014; revised December 16, 2014; accepted January 3, 2015.

M.M. Rajan Singaravel and S. Arul Daniel are with the Department of Electrical and Electronics, National Institute of Technology, Tiruchirappalli, Tamilnadu-620015, India (rajan.nitt@gmail.com, daniel@nitt.edu, +91-0431-2513256).

I. INTRODUCTION

Zero net energy buildings which have its cumulative energy consumption being met by renewable energy sources installed within its precincts have become increasingly popular [1]. These distributed generators (DGs) require new power electronic interfaces and control strategies to improve the efficiency and quality [2, 3]. DG systems based on a single intermittent source, either photovoltaic (PV) or wind energy system are unreliable due to seasonal variations. DG systems consisting of two or more renewable sources have a higher reliability, due to the complementary nature of the resources [4, 5]. In such hybrid schemes, permanent magnet synchronous generators (PMSG) are generally employed, as they do not require any reactive power support. Further, PMSG can be driven directly by wind turbine, thereby avoiding a gear box arrangement which requires regular maintenance [6]. Moreover, PMSG can be operated in higher power factor and higher efficiency than other machines because of its self-excitation property [7].

Various possible combinations of hybrid PMSG-PV systems are illustrated in the literature. Earlier, a six-arm converter topology was attempted, in which the outputs of a PV array and wind generator were subjected to a boost operation through individual switches to match the DC bus voltage [8]. In [9], a hybrid wind-PV system along with battery was explained, in which both the sources were connected to a common DC bus through individual power converters, then the DC bus was connected to the utility grid through an inverter. Grid connected PMSG-PV hybrid system with battery backup was described in [10], where the DC link voltage was fixed to battery voltage, but the maximum power extraction from wind-driven PMSG was not performed. A grid connected hybrid system where the PV array and wind-driven PMSG were connected to a common DC link through a multi-input DC-DC converter was proposed earlier in [11]. A PMSG – PV hybrid system with multi-input DC- DC converter and multi-input inverter was also brought out in [12].

In all the above hybrid DG systems with PMSG-PV attempted so far, the system either had individual power converters for each of the sources or a battery backup. Further, each converter was controlled using complex algorithms for

This article has been accepted for publication in a future issue of this journal, but has not been fully edited. Content may change prior to final publication. Citation information: DOI 10.1109/TIE.2015.2399277, IEEE Transactions on Industrial Electronics

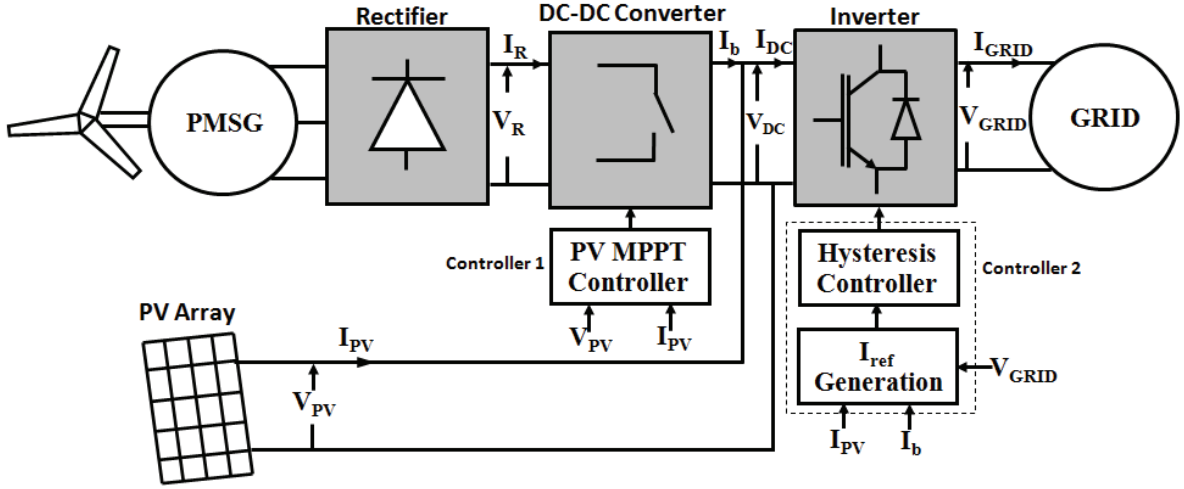

Fig. 1. Proposed DG system based on PMSG-PV sources

peak power tracking. In order to minimize the conduction and switching losses of the devices, it is necessary to have the minimum number of power converters (power conversion stages) and this has been attempted in this paper. In addition, it is desirable that power supplies in consumer sites employ fewer power electronic conversion stages in order to improve the overall efficiency. It should be noted that losses in conversion stages have to be compensated by increasing the sizes of the generators. This in turn increases the cost of hybrid generator. Generally, efficiency of DC-DC converter is maximum around 95 % when it is operated in full load condition [13]. Since source powers are varying, it is not always possible to operate the DC-DC converter at its maximum efficiency. In the above context, the proposed new topology avoids 5% loss in efficiency by eliminating an additional conversion stage.

Contrary to earlier schemes, the proposed hybrid generator has a PV array being directly connected to the DC link instead of being connected through a DC-DC converter. The DC link voltage is varied by a DC-DC converter interposed between the rectifier fed by PMSG and the grid connected inverter. The output voltage of the DC-DC converter forms the load line for the PV array. The inverter current is varied to extract maximum current from both the sources using current control strategy. The proposed topology could thus dispenses with a DC-DC converter, which in earlier schemes were connected after the PV array for maximum power extraction.

Two new controllers are attempted for the hybrid scheme proposed, in order to achieve the maximum power extraction from both the sources. A *d-q* axes model of the scheme has been developed and validated. The successful operation of this scheme in extracting maximum power from both the sources or from each of the sources has been established through simulation and experimental investigations. Further, the proposed scheme is also for employment by domestic consumers in a smart grid scenario, and hence maintenance free simple operation is envisaged. The proposed scheme is for a grid connected operation and hence battery storage is not necessary.

II. Description of the Scheme

The block diagram of proposed DG scheme is given in Fig.1, where a direct driven PMSG and a PV array are the sources. The PMSG output is rectified and fed into a DC-DC boost converter. The rectifier output voltage varies with the wind-speed. The PV array terminals are connected to the output of the DC-DC converter to form a common DC link for the proposed system. The inverter input terminals are tied to this common DC link. The PV array voltage (V_{PV}) is fixed to the output voltage of the DC-DC converter (V_{DC}) since the output terminals of both the PV array and the DC – DC converter are tied together. The output voltage of the DC-DC converter is automatically varied by a PV MPPT controller (Controller 1) to PV array's maximum power point voltage. Under this condition, the maximum current for the given irradiation is drawn from the PV array by the action of current controller (controller 2) of the inverter. The basic Perturb & Observe (P&O) algorithm [14, 15] is employed albeit with an inverted duty-cycle adjustment in controller 1. This revised adjustment in the proposed scheme is because of the DC-DC boost converter being fed by a stiff DC source (rectifier output) instead of the PV array. The operation of the controller with this revised duty-cycle variation is brought out in Section IV A. The output voltage of the current controlled inverter is tied to the grid voltage and the frequency and the phase requirement for synchronization are automatically met. The current fed to the grid by the inverter (I_{GRID}) follows the reference current signal (I_{ref}), which is automatically varied by controller 2 for drawing the maximum current from both PMSG & PV array. In the proposed scheme, the setting of DC voltage reference of the DC-DC converter to the peak power point voltage of the PV array and the reference current setting of current controlled inverter corresponding to the maximum current extractable from both the sources, results in peak power extraction from both the sources.

III. Model of the Proposed System

A model of the proposed DG system is developed to investigate the system performance. PMSG has been described by its steady state equivalent circuit and is shown in Fig. 2 [16]. The rectifier DC output voltage (V_R) and current (I_R) in terms of stator phase voltage V_S (rms) and stator current

This article has been accepted for publication in a future issue of this journal, but has not been fully edited. Content may change prior to final publication. Citation information: DOI 10.1109/TIE.2015.2399277, IEEE Transactions on Industrial Electronics

I_S(rms) are given as [16, 17];

$$V_R = \frac{3\sqrt{6}}{\pi} V_S , \quad (1)$$

$$I_R = \frac{\pi}{\sqrt{6}} I_S \quad (2)$$

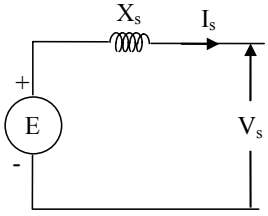

Fig. 2. Per-phase steady state equivalent circuit of PMSG

V_S varies with wind-speed and hence the rectifier output voltage V_R is a varying DC. This varying DC feeds the DC-DC converter. The output voltage of the DC-DC converter is given as

$$V_b = V_{DC} = V_R \frac{1}{1-\delta} \quad . \quad (3)$$

The DC link current is

$$I_{DC} = I_b + I_{pv} , \quad (4)$$

and the PV array current (I_{PV}) is given by [5]

$$I_{PV} = I_{SC} - I_d \quad (5)$$

where $I_d = 10^{-9} I_{SC} \left(\exp \frac{20.7}{V_{OC}} (V_{PV} + R_{se} I_{PV}) \right)$. (6)

The *d*-axis and *q*-axis voltage of the inverter are related with the DC link voltage as [18, 19],

$$v_d = V_{DC} g_d \quad (7)$$

$$v_q = V_{DC} g_q \quad (8)$$

where

$$g_d = \begin{bmatrix} \sum_{n=1,5,9...} \cos(n-1)\omega t - \sum_{n=3,7,11...} \cos(n+1)\omega t \\ + \left(\sum_{n=2,6,10...} \frac{1}{\sqrt{2}} \left\{ \cos\left[(n-1)\omega t - \frac{\pi}{4} \right] + \cos\left[(n+1)\omega t - \frac{3\pi}{4} \right] \right\} \right) \\ + \left(\sum_{n=4,8,12...} \frac{1}{\sqrt{2}} \left\{ \cos\left[(n-1)\omega t + \frac{\pi}{4} \right] - \cos\left[(n+1)\omega t - \frac{\pi}{4} \right] \right\} \right) \end{bmatrix} \quad (9)$$

$$g_q = \begin{bmatrix} \sum_{n=1,5,9...} \sin(n-1)\omega t - \sum_{n=3,7,11...} \sin(n+1)\omega t \\ + \left(\sum_{n=2,6,10...} \frac{1}{\sqrt{2}} \left\{ \cos\left[(n-1)\omega t - \frac{3\pi}{4} \right] + \cos\left[(n+1)\omega t - \frac{\pi}{4} \right] \right\} \right) \\ + \left(\sum_{n=4,8,12...} \frac{1}{\sqrt{2}} \left\{ \cos\left[(n-1)\omega t - \frac{\pi}{4} \right] + \cos\left[(n+1)\omega t - \frac{3\pi}{4} \right] \right\} \right) \end{bmatrix} . \quad (10)$$

Considering zero power loss in the inverter,

$$I_{DC} = \frac{1}{2} (i_d g_d + i_q g_q) . \quad (11)$$

Assuming zero power loss in DC-DC converter,

$$V_R I_R = V_b I_b \quad (12)$$

and $I_{DC} = I_b + I_{pv} = (1-\delta) I_R + I_{pv} = \frac{(1-\delta)\pi}{\sqrt{6}} I_S + I_{pv}$, (13)

where δ is duty-cycle of the DC-DC converter. The rectifier output (1) is connected to the models of DC – DC converter [20], PV array and the inverter. The *d* axis and *q* axis circuits of the system are shown in Fig. 3 and Fig. 4 respectively.

In the proposed scheme, δ and I_{ref} are varied to extract the maximum I_{DC} at any instant of time. Using Equations (1) – (13), the proposed DG system can be simulated on any platform. MATLAB has been employed to simulate the proposed scheme in this paper.

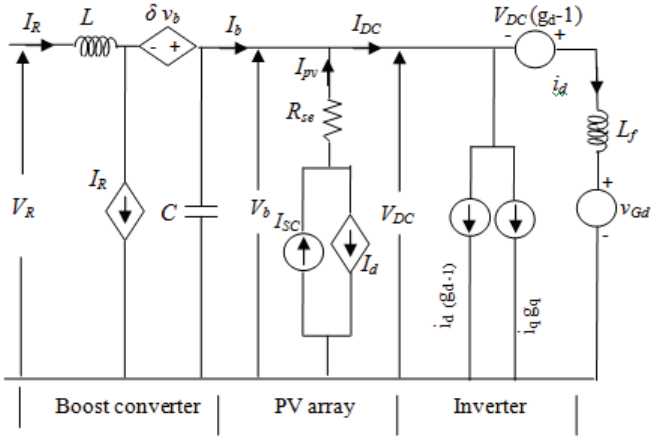

Fig. 3. d-axis equivalent of the system

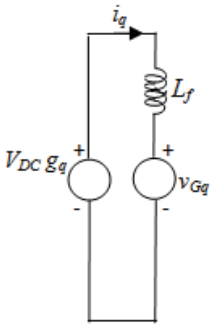

Fig. 4. q-axis equivalent of the system

IV. Operation of the Controllers

A. Case 1 (PV and PMSG generating power)

The wind and solar sources are generating power together in this case and the variation of duty-cycle of the DC-DC converter will eventually disturb the PV array's terminal voltage (since $V_{DC} = V_{PV}$). The rectifier voltage varies with the wind-speed and the duty-cycle of the boost converter needs to be automatically adjusted such that V_{DC} is equal to the peak power point voltage (V_m) of the PV array. At this point ($V_{PV} = V_{DC} = V_m$), the PV array delivers the maximum current (I_m) which is concurrently drawn by the current

This article has been accepted for publication in a future issue of this journal, but has not been fully edited. Content may change prior to final publication. Citation information: DOI 10.1109/TIE.2015.2399277, IEEE Transactions on Industrial Electronics

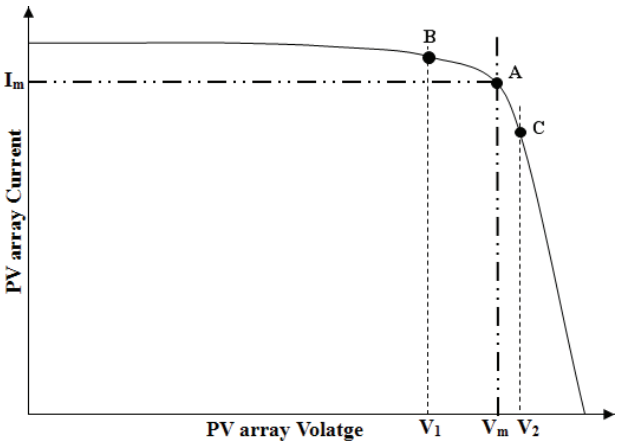

Fig. 5. IV curve of the PV array

controlled inverter. The operation of controller 1 is explained with the help of Fig. 5. As shown in the Fig. 5, the DC link voltage may be, say V_1 (B) or V_2 (C) depending upon the present duty-cycle of the DC–DC converter. To operate the PV array at its maximum power point (A), the DC-DC converter output (DC link voltage) is adjusted to V_m by varying the duty-cycle of the DC-DC converter by controller 1. The duty-cycle variation of controller 1 is given by

$$\delta_{new} = \delta_{old} + \text{sgn}(\Delta P)\text{sgn}(\Delta V_{PV})\Delta\delta \,, \qquad (14)$$

where $\Delta\delta$ is the perturbation in duty-cycle, sgn is Signum function. ΔP is the difference in PV array power and ΔV_{PV} is difference in PV array voltage before and after perturbation. If ΔP and ΔV_{PV} are both either positive or negative then the duty-cycle increases and vice-versa if different. The duty-cycle variation in this scheme is hence exactly opposite to the duty-cycle variation of a P&O controller used in existing schemes, where a PV array precedes a boost converter.

The main objective of controller 2 (Fig. 1) is to vary the inverter output current fed to the grid. The reference current (I_{ref}) for this hysteresis current controller is derived based on the available maximum power from the both the sources for a particular condition (i.e. irradiation and PMSG shaft torque). V_{PV}, is at maximum power point value by the action of controller 1. Current drawn from the boost converter (I_b) and PV (I_{PV}) together is maximized by changing I_{ref} as

$$I_{ref(new)} = I_{ref(old)} + \text{sgn}[\Delta(I_{PV} + I_b)]K \,, \qquad (15)$$

where $\Delta(I_{PV}+I_b)$ is the change in the sum of I_{PV} and I_b and K is the step in perturbation of I_{ref}. It is clear from (15), if current to be drawn from boost converter increases, I_{ref} also increases correspondingly. At steady-state, the reference current value for a particular condition of irradiation and wind speed is

$$I_{ref} = \sqrt{2}(V_{PV} I_{PV} + V_R I_R)/V_{GRID} \,. \qquad (16)$$

B. Case 2 (PMSG alone generating power)

It is obvious that during night time, the current transducer connected to the PV terminal will not give any response. In such a case, the controller 1 will skip the PV-MPPT algorithm and work in a voltage control mode. By taking the voltage transducer output (V_{DC}) as feedback signal, the controller 1 varies the duty-cycle of the boost converter to maintain the DC link voltage to a DC value corresponding to the rated RMS voltage of the grid. As I_{PV} is zero in this case, the controller 2 will keep adjusting the (I_{ref}) such that [by substituting $I_{PV} = 0$ in (15)]

$$I_{ref(new)} = I_{ref(old)} + \text{sgn}[\Delta(I_b)]K \qquad (17)$$

to extract the maximum power from the PMSG alone.

C. Case 3 (PV alone generating power)

When PMSG is not generating power, there is no input to the DC-DC converter and hence no triggering pulse is generated by controller 1. The controller 2 varies I_{ref} such that [by substituting $I_b = 0$ in (15)]

$$I_{ref(new)} = I_{ref(old)} + \text{sgn}[\Delta(I_{PV})]K \,, \qquad (18)$$

to feed the maximum power from PV array alone.

D. Composite operation of controllers

It is evident from all the three cases explained above, that controller 2 functions always to feed the maximum power either from both the sources or from any one of the sources to the grid by adjusting I_{ref}. On the other hand, controller 1 is idle when power is generated by PV alone. Different status of sources and the corresponding functions of two controllers are summarized in Table. I.

TABLE I
FUNCTIONS OF CONTROLLERS UNDER DIFFERENT CONDITIONS

Sources	Controller for DC-DC converter (Controller 1)	Hysteresis Controller (Controller 2)
PV and PMSG	Generates duty-cycle for PV array MPPT voltage	Generates current command to extract the maximum power from both the sources
PV alone	Triggering pulse not generated (Zero duty-cycle)	Generates current command to extract the maximum power from PV
PMSG alone	Generates duty-cycle to maintain constant DC link voltage*	Generates current command to extract the maximum power from PMSG

* Corresponding to the RMS voltage of the grid

V. Implementation of the Controllers

A. Controller for DC-DC Converter (Controller 1)

PIC 16F876A, a very low cost 16 bit microcontroller from MICROCHIP is used to implement the controller for the DC-DC converter. This controller gets feedback signals from a voltage transducer (LV20-P) and a current transducer (LA50-P) connected to the PV array terminals. The signals from these transducers are processed by signal conditioning circuits (SCC) and then connected to analog inputs of the microcontroller. These signals are digitized through internal Analog to Digital Conversion (ADC) module. The microcontroller is programmed to perform the MPPT algorithm for PV array based on (14). In built pulse width modulation (PWM) module of the microcontroller is enabled to produce the required PWM pulses for DC – DC converter.

This article has been accepted for publication in a future issue of this journal, but has not been fully edited. Content may change prior to final publication. Citation information: DOI 10.1109/TIE.2015.2399277, IEEE Transactions on Industrial Electronics

B. Hysteresis Current Controller (Controller 2)

The complete schematic of controller 2 is given in Fig. 6. High frequency op-amps (LM-318) are used to construct the hysteresis-current-controller. I_{PV} and I_b are sensed by the current transducers and digitized by the internal ADC module of the microcontroller. Based on (15), I_{ref} is determined and available as digital output from the microcontroller. This digital value is subsequently processed by a Digital to Analog Conversion (DAC) IC to obtain a DC value which corresponds to the peak value of I_{ref}. This DC value is multiplied with the sine wave reference extracted from the grid voltage, by a multiplier IC and fed to the hysteresis-current-controller as the reference current signal. When PV array (or PMSG) alone generates power, I_b (or I_{PV}) will be zero and I_{ref} is perturbed and adjusted automatically to extract the maximum power from PV array (or PMSG). When both the sources are generating, I_{ref} will be perturbed based on (15) and adjusted to maximize the DC link current I_{DC} for the corresponding irradiation and wind-speed conditions. As the sine wave reference is taken from the grid, the inverter output current will have grid frequency and will be in phase with the grid voltage.

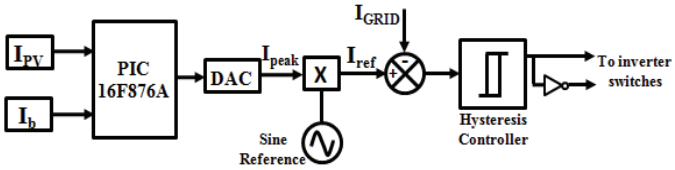

Fig. 6. Schematic of current reference generation with hysteresis controller (Controller 2 of Fig.1)

VI. SIMULATION AND EXPERIMENTAL VALIDATION

A single phase inverter was fabricated with the available IGBTs (SKM100GB125DN) for the laboratory prototype of the proposed hybrid generator. Firing pulses from hysteresis controller were given to IGBTs through a gate driver module (SKHI22AR). A DC – DC boost converter was also fabricated with a IGBT (CT60AM) and a hyper fast diode (RHRG30120). The pulses from the microcontroller were given to the IGBT through the gate driver (HCPL 3101). A PMSG [Rated power = 0.75 p.u., 12 pole, Speed = 1 p.u., Y – connected] and PV array consisting of 6 panels in series [Open circuit voltage (V_{OC}) = 0.22 p.u., Short circuit current (I_{SC}) = 0.47 p.u., peak power 0.08 p.u. for each panel] were chosen for both simulation and experimental investigations. The base values for the above mentioned per unit quantities as well as for graphs are given as follows: Base power = 1 kVA; Base Voltage = 100 V; Base current = 10 A; Base Speed = 500 rpm.

A. Steady-state investigations

The PMSG was driven by a DC motor to simulate the wind turbine. As PMSG and PV array voltage levels were chosen to be less than the grid voltage, a step-up transformer was used to connect the proposed DG system to the grid.

The steady-state DC link voltage and current along with the simulated waveforms (Irradiation = 500 W/m^2, PMSG shaft speed = 0.55 p.u.) are shown in Fig. 7.

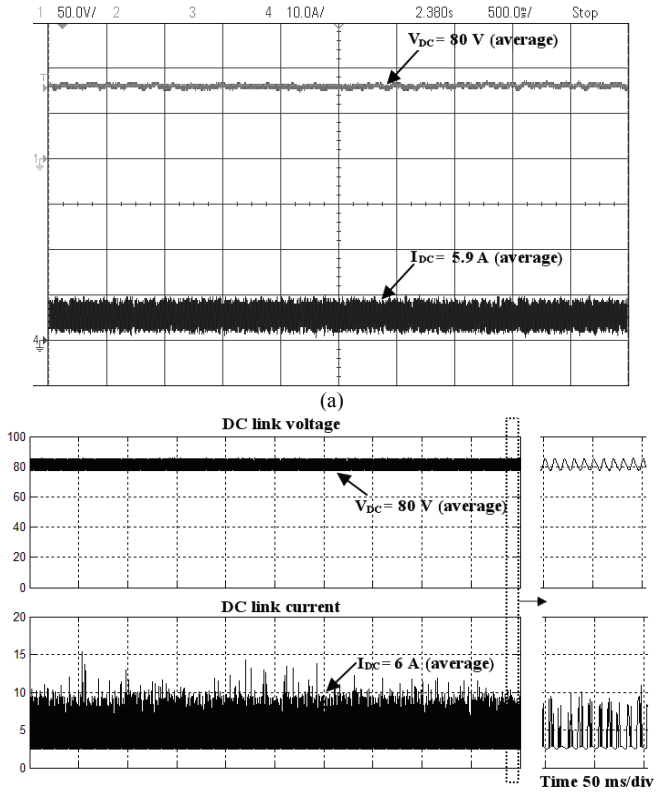

Fig. 7. DC link steady state waveforms
(a) Experimental (Voltage-50V/div, Current-10A/div, Time-500ms/div)
(b) Simulated (Voltage-20V/div, Current-5A/div, Time-500ms/div)

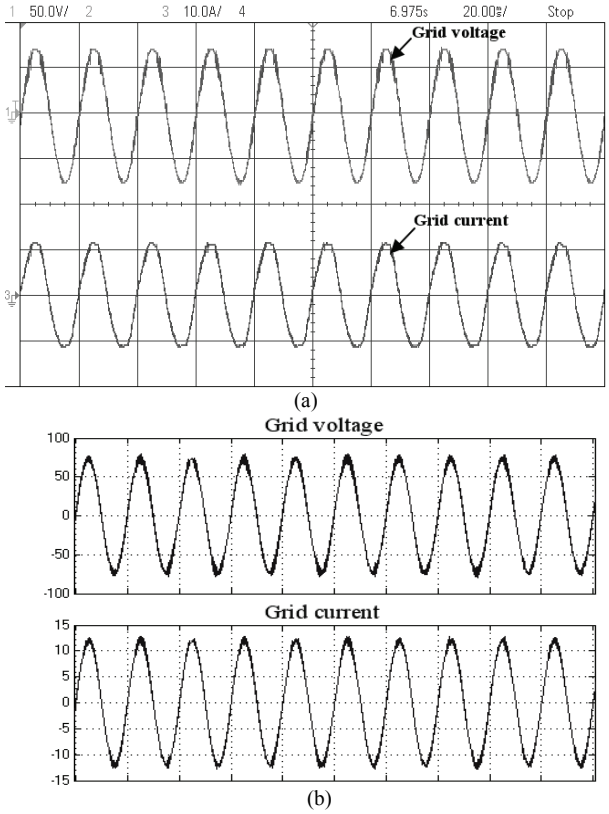

Fig. 8. Steady-state grid voltage and current waveforms
(a) Experimental(Voltage-50V/div, Current-10A/div,Time-20ms/div)
(b) Simulated (Voltage-50V/div, Current-5A/div, Time-20ms/div)

This article has been accepted for publication in a future issue of this journal, but has not been fully edited. Content may change prior to final publication. Citation information: DOI 10.1109/TIE.2015.2399277, IEEE Transactions on Industrial Electronics

The corresponding voltage and the current waveforms at grid side are also shown in Fig. 8 along with its simulated waveforms. It is clear from Fig. 8 that current was delivered to the grid by the inverter at unity power factor

B. Transients during a step change in shaft-speed

At constant irradiation of 650 W/m^2, a step increase in DC motor speed (from 0.4 p.u. to 0.8 p.u.) was applied. Consequently, the rectifier average output voltage had increased (from 28 V to 48.5 V) and the duty- cycle of the boost converter was found to have decreased (from 65 % to 40 %) to maintain the DC link voltage at the same level, so as to operate the PV array at its maximum power point. These changes in rectifier voltage level and duty-cycle of boost converter for a step increase in PMSG shaft speed are clearly depicted in Fig. 9 (a). From Fig. 9 (b), it is clear that, the DC link voltage is maintained at the same level (81 V) in order to extract the maximum power from PV array. However, it should be noted that the average DC link current had increased (from 4.7 A to 8.4 A) so as to extract the available increase in power from PMSG by the action of controller 2. The reference current magnitude (peak) was therefore found to have increased (from 10 A to 18 A) with this step-change in the shaft speed, thereby resulting in corresponding increase in the power delivered to the grid. The change in grid current under this condition is shown in Fig. 9 (c). It is clear from Fig. 9 that both the controller 1 and controller 2 react quickly for a step change in PMSG speed.

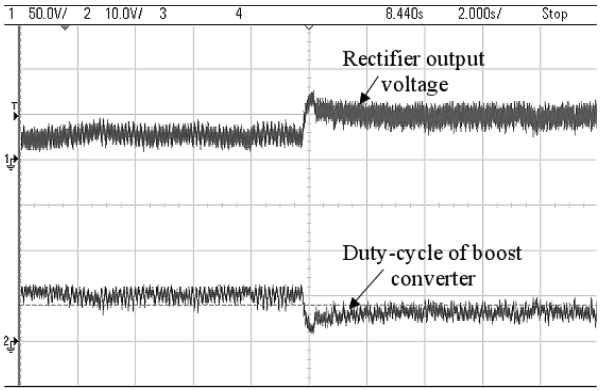

Experimental (Voltage 50V/div, Duty-cycle 0.6/div, Time 2s/div)

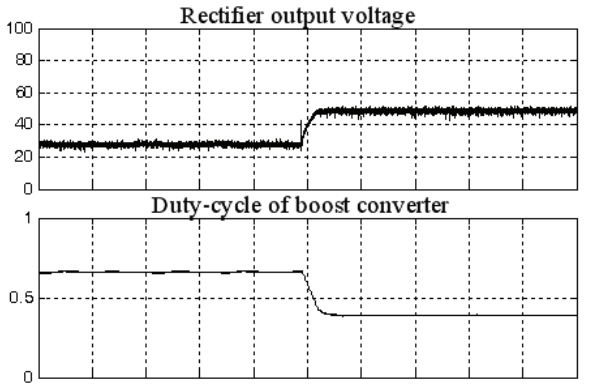

Simulated (Voltage 20V/div, Duty-cycle 0.5/div, Time 2s/div)

(a) Changes in rectifier output voltage and duty-cycle of boost converter

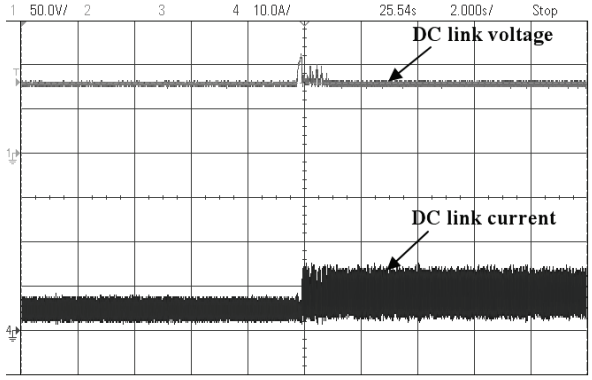

Experimental (Voltage 50V/div, Current 10 A/div, Time 2s/div)

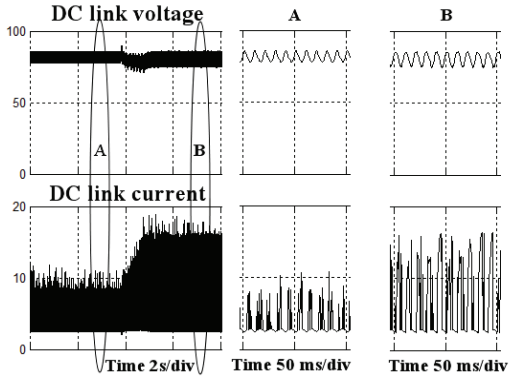

Simulated (Voltage 50V/div, Current 10/div)

(b) Changes in DC link voltage and current

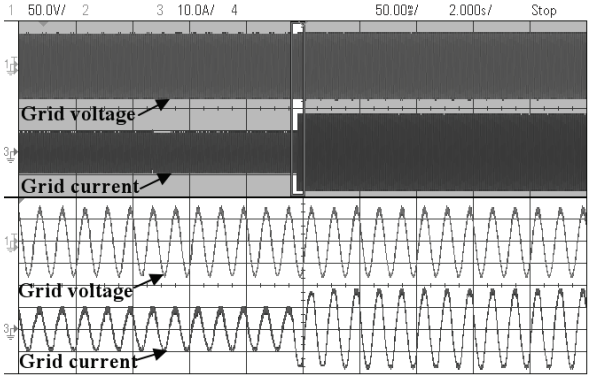

Experimental (Voltage 50V/div, Current 10A/div, Time 2s/div)

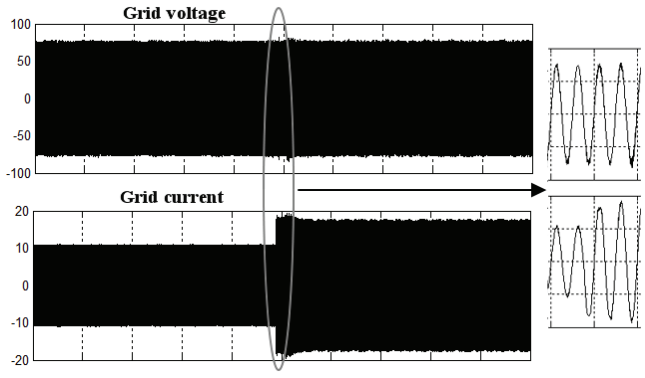

Simulated (Voltage 50V/div, Current 10A/div, Time 2s/div)

(c) Changes in grid current

Fig. 9 Transient response for a step change in PMSG shaft-speed

This article has been accepted for publication in a future issue of this journal, but has not been fully edited. Content may change prior to final publication. Citation information: DOI 10.1109/TIE.2015.2399277, IEEE Transactions on Industrial Electronics

It is evident from Figs. 7-9 that the simulated and experimental results resemble each other very closely and this validates the simulation.

C. Investigations on MPPT operation

In order to ascertain the successful operation of the hybrid generator for different irradiation and PMSG shaft-speed conditions, the following investigations were carried out in the laboratory prototype.

The experimentation was conducted when the irradiation has been constant without major variations. The PV array's open circuit voltage V_{OC} = 1.1 p.u. and short circuit current I_{SC} = 0.2 p.u. were constant during this short time-period. The DC motor speed was varied between 0.4 p.u. and 0.95 p.u. and the corresponding PMSG power, boost converter duty-cycle and current reference (i.e. the current fed to the grid) were noted down. The variations of these parameters with respect to DC motor speed (PMSG speed) is depicted in Fig. 10 (a). It is clear from Fig. 10 (a), that when PMSG shaft-speed had increased, the PMSG output power also had correspondingly increased and the current reference generated by the controller 2 also had increased proportionally in order to extract the available maximum power. As DC motor speed increases, the input voltage to the DC – DC converter also increases and hence, the duty-cycle of the boost converter automatically decreases to maintain the DC link voltage to the PV's maximum power point voltage.

Observations were also noted by maintaining the DC motor speed at 0.6 p.u., for a varying irradiation from 7:00 am to 5:00 pm. The I_{SC} of the PV array is directly proportional to irradiation. Hence, the variation of; PV power, duty-cycle of the boost converter and reference current, with variation of I_{SC} (instead of irradiation) are given in Fig. 10 (b). It can be found when I_{SC} (irradiation) increases, voltage corresponding to its maximum power point also increases and the duty-cycle of the boost converter correspondingly increases to match the maximum power point voltage of the PV array. At the same time, the reference current value also proportionally increases to extract the available maximum power from both the sources as expected.

With the variations in irradiation, the corresponding variations in V_{OC} is not as significant as compared to the variations of the I_{SC} of the PV array. Hence, the duty-cycle variation of the DC-DC converter is over a small band [Fig. 10(b)] for wide variations in irradiation.

In order to further ascertain the operation of the controller in tracking the peak power from both the sources, the simulated peak power available and the peak power extracted from the experimental test rig were compared for various conditions and presented in Fig. 11. Close conformity of the experimental peak powers with simulated peak powers of both the sources under varying wind speed (PMSG shaft speed) and irradiation (I_{SC}) confirms adequately the successful operation of the controllers.

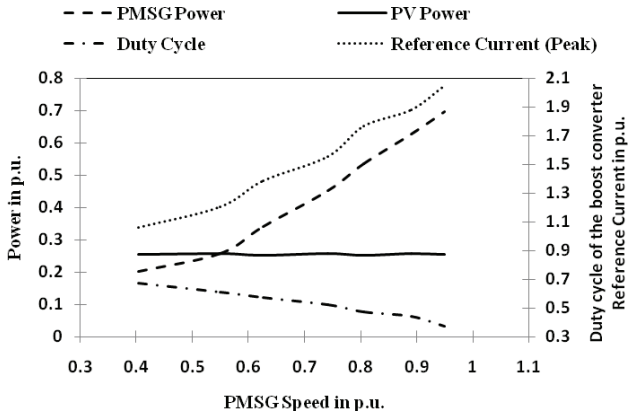

(a)

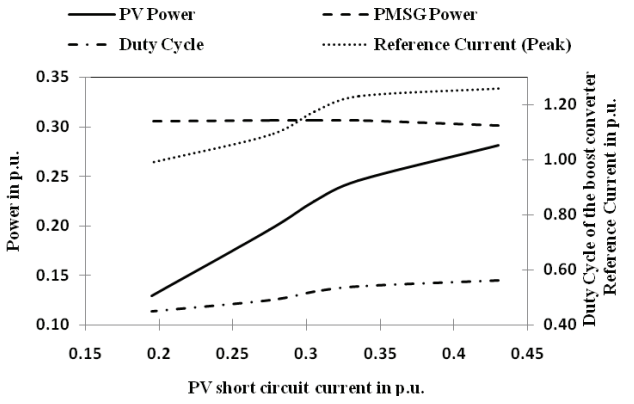

(b)

Fig. 10. Generator power variations with PMSG shaft-speed and irradiation
(a) PMSG Power, Boost converter duty-cycle, Reference current variation with PMSG shaft speed
(b) PV Power, Boost converter duty-cycle, Reference current variation with I_{SC} of the PV array

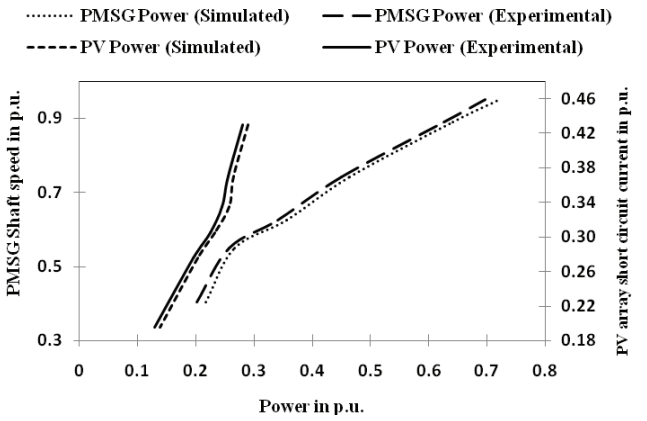

Fig. 11. Comparison of maximum power available (simulation) and the power delivered by the laboratory prototype

D. Total harmonic distortion

The total harmonic distortion (THD) of the voltage and the current at grid side were measured by using power quality analyzer and the results are shown in Fig. 12. It can also be noted from Fig. 12 that voltage and current THD are 1.8 % and 4.6 % respectively which are below the allowable THD recommended by IEEE for interconnecting distributed resources with utility.

This article has been accepted for publication in a future issue of this journal, but has not been fully edited. Content may change prior to final publication. Citation information: DOI 10.1109/TIE.2015.2399277, IEEE Transactions on Industrial Electronics

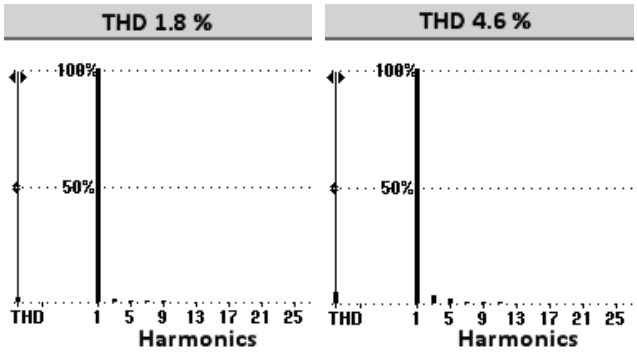

(a) (b)

Fig. 12. THD at grid side
(a) Voltage THD
(b) Current THD

VII. CONCLUSIONS

A new reliable hybrid DG system based on PV and wind-driven PMSG as sources, with only a boost converter followed by an inverter stage, has been successfully implemented. The mathematical model developed for the proposed DG scheme has been used to study the system performance in MATLAB. The investigations carried out in a laboratory prototype for different irradiations and PMSG shaft speeds amply confirm the utility of the proposed hybrid generator in zero net energy buildings. In addition, it has been established through experimentation and simulation that the two controllers, digital MPPT controller and hysteresis-current-controller which are designed specifically for the proposed system have exactly tracked the maximum powers from both the sources.

Maintenance free operation, reliability and low cost are the features required for the DG employed in secondary distribution system. It is for this reason, the developed controllers employ very low cost microcontrollers and analog circuitry. Further, the results of experimental investigations are found to be matching closely with the simulation results there by validating the developed model. The steady state waveforms captured at grid-side show that power generated by the DG system is fed to the grid at unity power factor. The voltage THD and the current THD of the generator meet the required power quality norms recommended by IEEE. The proposed scheme easily finds application for erection at domestic consumer sites in a smart grid scenario.

REFERENCES

[1] J.Byun, S.Park, B.Kang, I.Hong, S.Park, "Design and implementation of an intelligent energy saving system based on standby power reduction for a future zero-energy home environment", *IEEE Trans. Consum. Electron.,* vol.59, no. 3, pp.507-514, Oct. 2013.

[2] Jinwei He, Yun Wei Li, Blaabjerg, F., "Flexible Microgrid Power Quality Enhancement Using Adaptive Hybrid Voltage and Current Controller," *IEEE Trans. Ind. Electron.*, vol.61, no.6, pp.2784-2794, June 2014

[3] Weiwei Li, Xinbo Ruan, Chenlei Bao, Donghua Pan, Xuehua Wang, "Grid Synchronization Systems of Three-Phase Grid-Connected Power Converters: A Complex-Vector-Filter Perspective," *IEEE Trans. Ind. Electron.,* vol.61, no.4, pp.1855-1870, April 2014.

[4] C. Liu, K.T. Chau, X. Zhang, "An Efficient Wind-Photovoltaic Hybrid Generation System Using Doubly Excited Permanent-Magnet Brushless Machine", *IEEE Trans.Ind.Electron*,vol.57, no.3, pp.831-839,Mar.2010.

[5] S. Arul Daniel, N. Ammasai Gounden, "A novel hybrid isolated generating system based on PV fed inverter-assisted wind-driven induction Generators," *IEEE Trans. Energy Convers*., vol. 19, no. 2, pp.416-422, June 2004.

[6] H. Polinder, F. F. A. van der Pijl, G. J. de Vilder, and P. J. Tavner, "Comparison of direct-drive and geared generator concepts for wind turbines," *IEEE Trans. Energy Convers*., vol. 21, no. 3, pp.725–733, Sep 2006.

[7] C. N. Bhende, S. Mishra, Siva Ganesh Malla, "Permanent Magnet Synchronous Generator-Based Standalone Wind Energy Supply System" *IEEE Trans. Sustain. Energy*, vol. 2, no. 4, pp. 361-373, Oct 2011.

[8] H.C. Chiang, T.T. Ma, Y.H. Cheng, J.M. Chang, W.N. Chang, "Design and implementation of a hybrid regenerative power system combining grid-tie and uninterruptible power supply functions," *IET Renewable Power Generation,* 2010, vol. 4, no. 1, pp.85,99, 2010.

[9] S-K. Kim, J-H. Jeon, C-H. Cho, J-B. Ahn, S-H. Kwon, "Dynamic Modeling and Control of a Grid-Connected Hybrid Generation System With Versatile Power Transfer," *IEEE Trans. Ind. Electron.*, vol. 55, no. 4, pp.1677-1688, April 2008.

[10] Francois Giraud, Ziyad M. Salameh, "Steady-State Performance of a Grid-Connected Rooftop Hybrid Wind-Photovoltaic Power System with Battery Storage",*IEEE Trans. Energy Convers*., vol.16 , no. 1, pp.1-7, Mar. 2001.

[11] Sungwoo Bae, Alexis Kwasinski, " Dynamic Modeling and Operation Strategy for a Microgrid with Wind and Photovoltaic Resources", *IEEE Trans. Smart Grid*, vol. 3, no. 4, pp. 1867 -1876, Dec. 2012.

[12] Y-M. Chen, Y-C. Liu, S-C. Hung, C-S. Cheng, "Multi-Input Inverter for Grid Connected Hybrid PV/Wind Power Systems", *IEEE Trans. Power Electron.*, vol. 22, no. 3, pp. 1070-1077, May 2007.

[13] Byung-Duk Min; Jong-Pil Lee; Jong-Hyun Kim; Tae-Jin Kim; Dong-Wook Yoo; Eui-Ho Song, "A New Topology With High Efficiency Throughout All Load Range for Photovoltaic PCS", *IEEE Trans. Ind. Electron.,* vol. 56, no. 11, pp.4427-4435, Nov. 2009.

[14] B. Subudhi, R. Pradhan, "A Comparative Study on Maximum Power Point Tracking Techniques for Photovoltaic Power Systems," *IEEE Trans. Sustain. Energy.* vol. 4, no. 1, pp.89-98, Jan 2013.

[15] M.A.G de Brito, L Galotto, L.P. Sampaio, Guilherme de Azevedo e Melo, C.A. Canesin, "Evaluation of the Main MPPT Techniques for Photovoltaic Applications," *IEEE Trans. Ind. Electron,* vol. 60, no. 3, pp.1156-1167, Mar. 2013.

[16] S. A. Daniel, K. Pandiraj, N. Jenkins, "Control of an integrated wind-turbine generator and photovoltaic system for battery charging", in *Proc. British Wind Energy Conf.,* 1997, pp. 121-128.

[17] N.Mohan, T.M. Undeland, W.P.Robbins: "Power Electronics: Converter, Application and Design", New Delhi: Wiley India, 2007.

[18] R. Zhang, M. Cardinal, P. Szczesny, M. Dame, "A Grid Simulator with Control of Single-Phase Power Converters in D-Q Rotating Frame", in *Proc. 33rd Annual IEEE Power Electronics Specialists Conf.,* 2002, pp. 1431-1436.

[19] M. Gonzalez, V. Cárdenas, F. Pazos, "DQ transformation development for single-phase systems to compensate harmonic distortion and reactive power," in *Proc. 9th IEEE Int. Power Electronics Congress, 2004*, pp.177-182.

[20] M. Arutchelvi, S. Arul Daniel, "Voltage Control of an Autonomous Hybrid Generation Scheme Based on PV Array and Wind – Driven Induction Generators", *Electric Power Components and Systems*, vol. 34, no. 7, pp.759 – 773, June 2006.

M. M. Rajan Singaravel completed his B.Tech. Electrical and Electronic Engineering from SASTRA University in 2008 and completed M.E. Power Electronics and Drives from P.S.G. College of Technology, Coimbatore (Anna University) in 2010. Currently he is pursuing his Ph.D. in NIT, Tiruchirappalli. His interests are battery storage systems, hybrid wind-solar systems and power electronics for renewable systems.

S. Arul Daniel received the B.E. degree from the GCT, Coimbatore, India, in 1988, and the M.E. and Ph.D. degrees from REC, Tiruchirappalli (Bharathidasan University), India, in 1991 and 2003, respectively. He is with the Department of Electrical and Electronics Engineering, NIT, Tiruchirappalli, since 1994, where he is currently a professor. His areas of interest include distribution system, hybrid renewable energy systems, distributed generation and micro-grids.